

Practical Methodology for the Inclusion of Nonlinear Slosh Damping in the Stability Analysis of Liquid-propelled Space Vehicles

John A. Ottander*

Dynamics Concepts Inc., Jacobs ESSSA Group, Huntsville, AL 35806 USA

Robert A. Hall†

CRM Solutions, Jacobs ESSSA Group, Huntsville, AL 35802 USA

J. F. Powers ‡

National Aeronautics and Space Agency, Marshall Space Flight Center, Huntsville, AL 35812 USA

A method is presented that allows for the prediction of the magnitude of limit cycles due to adverse control-slosh interaction in liquid propelled space vehicles using non-linear slosh damping. Such a method is an alternative to the industry practice of assuming linear damping and relying on: mechanical slosh baffles to achieve desired stability margins; accepting minimal slosh stability margins; or time domain non-linear analysis to accept time periods of poor stability. Sinusoidal input describing functional analysis is used to develop a relationship between the non-linear slosh damping and an equivalent linear damping at a given slosh amplitude. In addition, a more accurate analytical prediction of the danger zone for slosh mass locations in a vehicle under proportional and derivative attitude control is presented. This method is used in the control-slosh stability analysis of the NASA Space Launch System.

Nomenclature

Z	displacement of vehicle c.g. normal (m)
Z_{zj}	sloshing fluid displacement in jth tank (m)
β_E	engine angle (rad)
ϕ	angle of vehicle centerline (rad)
a_0	attitude control gain (-)
a_1	attitude-rate control gain (-)
c_2	$R'X_{c.g.}/I$ ($1/s^2$)
D	drag force (N)
F	total engine thrust (N)
I	pitch-yaw vehicle moment of inertia with engines and sloshing fluid (kg-m ²)
k_3	F/M (m/rad-s ²)
k_4	R'/M (m/rad-s ²)
l_{sj}	c.g.-to-slosh mass distance = $X_{c.g.} - X_{sj}$ (m)
$l_{c.p.}$	center of percussion = $I/(MX_{c.g.})$ (m)
M	vehicle mass with engines and sloshing fluid (kg)
m_{sj}	slosh mass, jth tank (kg)
R'	vectored engine thrust (N)
$X_{c.g.}$	center of gravity measured from gimbal (m)

*Aerospace Engineer

†Aerospace Engineer

‡Aerospace Engineer

X_{sj}	slosh mass location measured from gimbal (m)
ξ_{sj}	slosh equivalent linear damping, jth tank (-)
ω_{sj}	slosh natural frequency, jth tank (rad/s)
α_{sj}	slosh damping slope, jth tank (1/m)
s	complex Laplace variable

I. Introduction

LIQUID propelled space vehicles, especially the stages of launch vehicles, are often over 90% propellant by mass. This high propellant mass fraction is necessary in order to maximize the payload that can be delivered to the desired trajectory state. The motion of the liquid propellant inside of the tanks can significantly affect the flight control stability and performance as most recently demonstrated by the failure of Flight 2 of the Space X Falcon 1 rocket in 2007. During Flight 2, the first stage burn was successful but approximately 90s into the burn of the second stage, a large limit cycle developed in the pitch and yaw axis due to control interaction with the liquid oxygen tank which led to pre-mature engine shutdown. The corrective action after Flight 2, was to add ring slosh baffles to the tank to increase the damping of the slosh mode. The use of tank baffles is a traditional technique to increase damping of the slosh motion and was used on both the Saturn V and the Space Shuttle. However, the mass impact of adding baffles reduces the vehicle trajectory performance and there is continual desire to minimize their use.

For flight control, the primary liquid motion of concern is the first lateral slosh mode of the liquid surface. As described in Abramson² and Dodge³ this motion can be described with a mechanical model of either a spring-mass-damper or a pendulum with viscous friction attached at a certain location inside the tank (figure 1). Just as the pendulum model natural frequency ($\omega_n = \sqrt{g/l}$) increases with the vertical acceleration (g) and decreases with length (l), the slosh mode natural frequency increases with vertical acceleration, and decreases with tank diameter. The natural frequencies of slosh modes in large diameter tanks in launch vehicles can be 0.5 Hz or lower. The rule of thumb is that the simple slosh analogue mechanical models become less valid when slosh displacement magnitude exceeds 10%-15% of the tank radius.

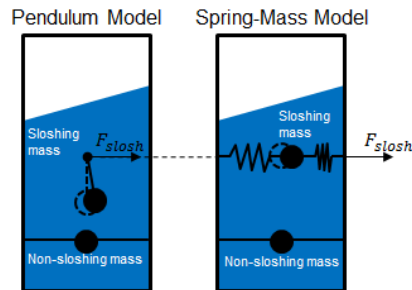


Figure 1. Mechanical analogues for lateral slosh motion

For cylindrical tanks, slosh mass, location, natural frequency, and damping can be predicted using analytical and empirical relationships.² A well known empirical relationship for slosh damping in a baffled tank is given by Miles.⁴ Often sub-scale ground testing is done to validate or adjust predictions. Recently, Computational Fluid Dynamics (CFD) has also been used in conjunction with sub-scale testing to develop better predictions of slosh parameters.⁵ A key result is that the effective damping coefficient increases as a function of slosh motion magnitude due to increased fluid energy dissipation with larger motions even at amplitudes well within the validity range of the simple mechanical analogue models.

The possibility of adverse control-slosh interaction has been known to control system designers since the beginning of the space age in the 1950s. The primary control system impact of such an instability is increased usage of the thrust vector control (TVC) with potential saturation or duty cycle violations possible. For cryogenic fluids, large slosh motion can cause droplet formation which greatly increase the heat transfer to the liquid from the warmer pressurized gas in the ullage space. The cooling of the ullage can cause increased

pressurization system usage and ullage collapse.

If the slosh frequency is sufficiently separated from the control frequency, instability can be prevented through filtering, but the control bandwidth will often be in proximity to the slosh frequencies due to performance needs and other dynamics (Lee⁶ and Frosch⁷).

One of the well known results discussed in Bauer⁸ and Greensite⁹ is that for an attitude control system with attitude and attitude rate feedback (i.e. PD control) with a single dominant slosh mass, only slosh mass locations between the vehicle CG and the vehicle center of percussion are destabilizing. For higher order systems with multiple tanks, some of whose frequencies are close enough proximity to dynamically couple, the result no longer fully holds, but through practice it has been shown to be a good guideline for which slosh tanks may need baffles for extra damping.

There has been research on the use of mechanical models which better represent the non-linear fluid dynamics at high amplitudes such as Bauer¹⁰ in which a 2-D model of a mass constrained to a parabolic surface was introduced. In addition, the coupling of non-linear fluid equations of motions with spacecraft motion has been investigated by Peterson.¹¹ Although these investigations do include non-linear effects in the equations of motion they ignored the non-linear effects on fluid damping. Non-linear adaptive control using neural networks has been applied to a spacecraft with slosh,¹² again the non-linear nature of slosh damping was not considered.

The traditional launch vehicle control approach is to use a linear control system and achieve a gain and phase margin of 6 dB and 30 deg respectively (see Dennehy¹³ and Frosch⁷) assuming a prescribed amount of slosh damping, invariant of amplitude. Using this criteria, slosh baffle requirement can be generated, which can be performed with automated numerical search routines as in Orr.¹⁴ Due to the undesirable mass penalty of large baffles, several launch vehicles which have been operational, have accepted lower stability margins for slosh than the standard 6dB/30deg in order to minimize baffle mass. Additional analysis to support this decision involve the use of dispersed time-varying non-linear six degree of freedom (6DOF) simulations as well as time to double analysis of any time periods of negative margin during flight. Since propellant is continually consumed during flight and the mass properties are continually changing, an argument can be made to accept unstable slosh-control interaction as long as the time period during which it occurs is short enough that no significant slosh motion can result. There is a general lack published literature of this practice and there are no generally agreed upon guidelines for using slosh stability margin criteria below the standard 6db/30deg.

In the traditional linear analysis, a slosh amplitude (wave height) is assumed for determining the linear damping. This amplitude is a key assumption since it can strongly affect the impact slosh has on the linear stability analysis. For example a choice of a very small slosh amplitude will result in small damping which can cause poor or negative stability margins, while the choice of a larger slosh amplitude will result in greater damping which can make stability margins appear ample.

The method presented in this paper is to augment the traditional linear approaches by using the non-linear damping profile as part of the linear control system analysis. Central to the nonlinear analysis is the assessment of the amplitude of the inevitable TVC-slosh limit cycle which will occur under degraded margin conditions for a slosh mass in the "danger zone". This amplitude can then be used as a meaningful criteria for accepting a given baffle design. The method remains highly practical as a standard analysis method since it is still largely based upon linear-time-invariant (LTI) modeling, by computing several key transfer functions over a range of wave heights for a particular trajectory analysis point. This method has recently been adopted by the MSFC control systems design & analysis branch in the evaluation of the slosh stability of the SLS core stage tanks.

This paper is organized into 3 sections. The first section lays out the system equations, the description of the non-linear damping, and example parameters for a hypothetical large upper stage. The next section discusses why slosh can be destabilizing for a vehicle under attitude control and derives a updated "danger zone" for slosh mass location. The third section describes the limit cycle analysis method and presents results for the example system.

A. System Equations

1. Plant Dynamics

The systems equations of motions for a liquid rocket controlled by vectoring thrust R' at the aft of the vehicle through gimballed engines (see figure 2), with n sloshing tanks represented using the spring-mass-damper

model are here presented. The equations are based on the linearized planar equations of motions presented in Frosch⁷ which were used for control design and analysis of the Saturn V S-IC stage. Dynamics not needed which were removed to simplify the system include structural dynamics, aerodynamics, nozzle dynamics, and sensor dynamics. These dynamics are not needed in order to show the impact of slosh on stability, but when included these dynamics do constrain the control design sufficiently to often force the main control frequency to be in proximity to slosh modes.

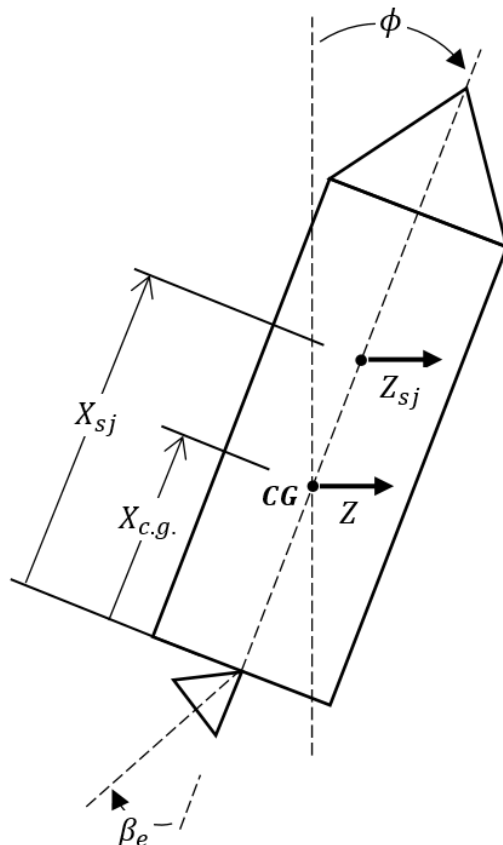


Figure 2. Space vehicle diagram with gimbaled thrust vector and slosh mass

$$\phi s^2 = -c_2 \beta_e - \frac{1}{I} \sum_{j=1}^n m_{sj} (l_{sj} s^2 + k_3) Z_{sj} \quad (1)$$

$$Z s^2 = k_4 \beta + k_3 \phi - \frac{1}{M} \sum_{j=1}^n m_{sj} Z_{sj} s^2 \quad (2)$$

$$(s^2 + 2\xi_{sj} \omega_{sj} + \omega_{sj}^2) Z_{sj} = -Z s^2 + (l_{sj} s^2 + k_3) \phi \quad (3)$$

The transfer function equations of motion are converted to state space form, assuming only a single slosh mass. A matrix E represents the coupled mass matrix and is numerically inverted prior to the computation of the final state space equations. The outputs of the state space equations used for control are the attitude angle and rate of the vehicle.

$$E \dot{x} = A' x + B' u \quad (4)$$

$$\dot{x} = (E^{-1} A') x + (E^{-1} B') u \quad (5)$$

$$y = C x \quad (6)$$

$$x = \begin{bmatrix} z \\ \phi \\ z_{s1} \\ \dot{z} \\ \dot{\phi} \\ \dot{z}_{s1} \end{bmatrix} \quad (7)$$

$$u = \beta_e \quad (8)$$

$$E = \begin{bmatrix} 1 & 0 & 0 & 0 & 0 & 0 \\ 0 & 1 & 0 & 0 & 0 & 0 \\ 0 & 0 & 1 & 0 & 0 & 0 \\ 0 & 0 & 0 & 1 & 0 & \frac{m_{s1}}{M} \\ 0 & 0 & 0 & 0 & 1 & -\frac{m_{s1}l_{sj}}{I} \\ 0 & 0 & 0 & 1 & -l_{s1} & 1 \end{bmatrix} \quad (9)$$

$$A' = \begin{bmatrix} 0 & 0 & 0 & 1 & 0 & 0 \\ 0 & 0 & 0 & 0 & 1 & 0 \\ 0 & 0 & 0 & 0 & 0 & 1 \\ 0 & k_3 & 0 & 1 & 0 & 0 \\ 0 & 0 & m_{s1}k_3/I & 0 & 0 & 0 \\ 0 & k_3 & \omega_{s1}^2 & 0 & 0 & -2\xi_{s1}\omega_{s1} \end{bmatrix} \quad (10)$$

$$B' = \begin{bmatrix} 0 \\ 0 \\ 0 \\ k_4 \\ -C_2 \\ 0 \end{bmatrix} \quad (11)$$

$$C = \begin{bmatrix} 0 & 1 & 0 & 0 & 0 & 0 \\ 0 & 0 & 0 & 0 & 1 & 0 \end{bmatrix} \quad (12)$$

2. Control System

In order to generate the minimal system which demonstrates the general slosh stability characteristics, the control system is simplified to be composed of attitude rate and attitude feedback only while sensor dynamics, actuator dynamics, internal delays, additional filtering for structural dynamics, and accelerometer feedback are omitted. The plant system and control system are connected to create the closed loop system. For open loop stability analysis, the loop is broken at the thrust vector angle β_e . Note that vehicle drift (z, \dot{z}) is not observable through the feedback variables, resulting in neutrally stable poles. Depending on the portion of flight, drift is either left uncontrolled or is controlled through accelerometer feedback and/or a much slower outer guidance loop not analyzed here, but they could be included without loss of generality or applicability, in fact, they are included in the the full SLS system with success.

$$\beta_e = -a_0\phi - a_1\dot{\phi} \quad (13)$$

3. Non-Linear Damping

In many applications the non-linear damping relationship is often experimentally computed using log decrement of free decay time histories from sub-scale testing or full scale CFD. However, the relationship can be derived if the form of the non-linear damping is known. For the purposes of this paper, let the non-linear damping relationship be a product of a constant b_1 and an odd square law of slosh mass velocity (\dot{z}_{sj}). This relationship is similar to drag in that it is proportional to the square of the velocity.

$$Acc_{d,nonlinear} = -b_{sj}\dot{z}_{sj}|\dot{z}_{sj}| \quad (14)$$

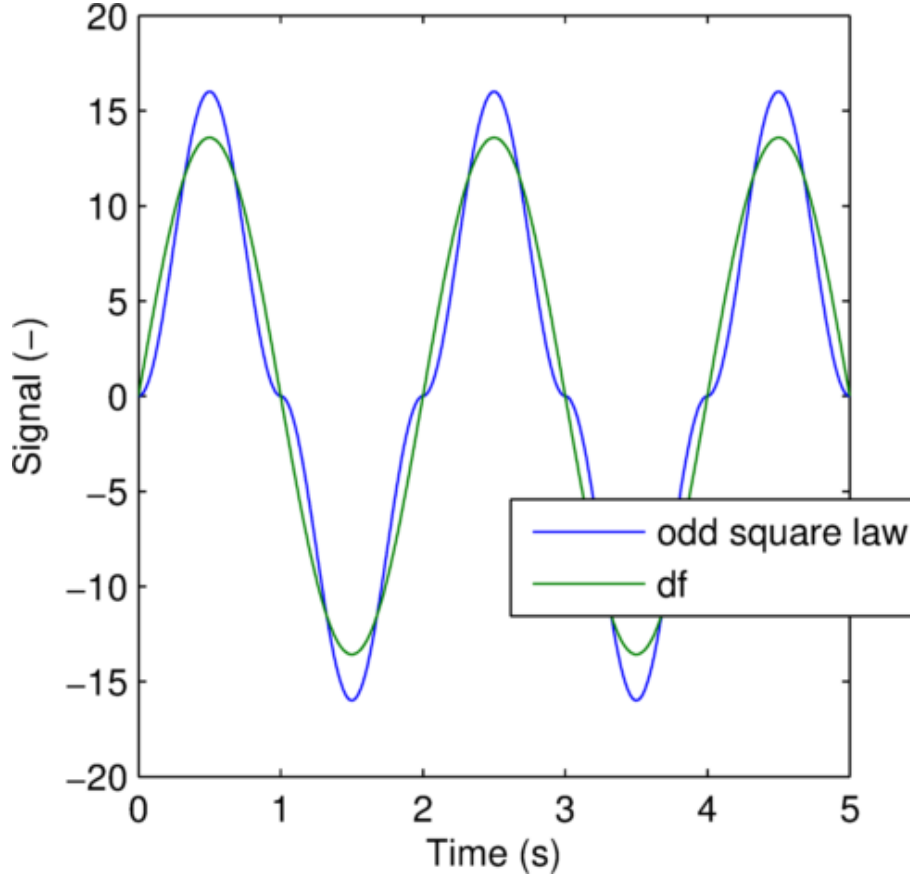


Figure 3. Odd square law and describing function for sinusoidal input

A describing function is a least-squares fit of a non-linear expression using linear terms for a specified input. The describing function for an odd square law ($y = x|x|$) with a sinusoidal input of amplitude A_x and frequency of Ω ($x = A_x \sin(\Omega t)$) is known to be $y = x \frac{8}{3\pi} A_x$ (Gelb¹⁵) and is depicted in figure 3. Using this describing function in Eq. (14) gives an expression as a function of the amplitude of the slosh displacement ($A_{z_{sj}}$) or slosh velocity ($A_{\dot{z}_{sj}}$).

$$Acc_{d,DF} = -b_{sj}\dot{z}_{sj}\frac{8}{3\pi}A_{\dot{z}_{sj}} \quad (15)$$

$$Acc_{d,DF} = -b_{sj}\dot{z}_{sj}\frac{8}{3\pi}\Omega A_{z_{sj}} \quad (16)$$

Assuming Ω is equal to ω_{sj} and setting the describing function expression equal to the expression for linear damping acceleration ($-2\omega_{sj}\xi_{sj}\dot{z}_{sj}$) allows ξ_{sj} to be solved for.

$$-b_{sj}\dot{z}_{sj}\frac{8}{3\pi}\Omega A_{z_{sj}} = -2\omega_{sj}\xi_{sj}\dot{z}_{sj} \quad (17)$$

$$\xi_{sj} = \left(\frac{b_{sj}}{2} \frac{8}{3\pi} \right) A_{z_{sj}} \quad (18)$$

Equation (18) shows that the equivalent linear damping of the odd square law damping is a linear function of the amplitude of oscillation. The same expression can also be derived based on the energy dissipation over a period of sinusoidal motion (Craig¹⁶). Let the slope of the above relationship be called α_{sj} .

$$\alpha_{sj} = \left(\frac{b_{sj}}{2} \frac{8}{3\pi} \right) \quad (19)$$

Assuming an equivalent damping as a function of slosh amplitude ($\xi_{sj} = f_{\xi_{sj}} A_{z_{sj}}$) has been defined (through test or other means). It has been found through practice, that Eq. (20) provides a practical approximation of the damping for use in time domain simulation, as long as $f_{\xi_{sj}}$ can be locally approximated as a linear function.

$$\xi_{sj} = \frac{3\pi}{8} f_{\xi_{sj}} \left(\frac{\dot{z}_{sj}}{\omega_{sj}} \right) \quad (20)$$

4. Example System Parameters

A set of parameters were chosen to represent a hypothetical large upper stage similar in size to the upper stages used on the Saturn V or the Space Launch System. The parameters chosen exhibit poor slosh phase characteristics and proximal frequencies that readily challenge flight control stability.

Table 1. Example System Parameters

Name	Value	Units
$F(= R')$	$9x10^5$	N
M	$1x6^4$	kg
I	$9x10^5$	kg-m ²
$X_{c.g.}$	6	m
X_{s1}	9	m
m_{s1}	$1x10^3$	kg
ω_{s1}	2	rad/s
α_{s1}	0.01	1/m
a_0	0.08	rad/rad
a_1	0.14	rad/(rad/s)

B. Slosh Location Sensitivity

As discussed previously, the "danger zone" observed in Bauer⁸ for an example system and derived in Green-site⁹ has the potential for slosh-control instability occurring when the slosh mass is located between the center of mass and the center of percussion. The stability bounds are derived from the equation of motion using the rules for a root locus. The root locus for the example system with slosh damping set to zero is given in figure 4. The four poles at the origin correspond to the two rotation poles and two translation poles. The real zero is a function of the PD control. The pair of imaginary axis poles and zeros are a result of the slosh motion coupling with the rotation and translation dynamics. Given the angles from a pole to all the other poles and zeros, the angle of departure of the root locus can be calculated with the well known root locus rule. For this configuration the root locus of the OL slosh poles will go to the right. The only way to stabilize this system, while under PD control, is to add intrinsic damping to the slosh to move the OL slosh poles into the left half of the plane to accommodate the destabilizing effect of the PD control. Following the angle of departure root locus rule, if the slosh pole was greater than the slosh zero, then root locus would be stable.

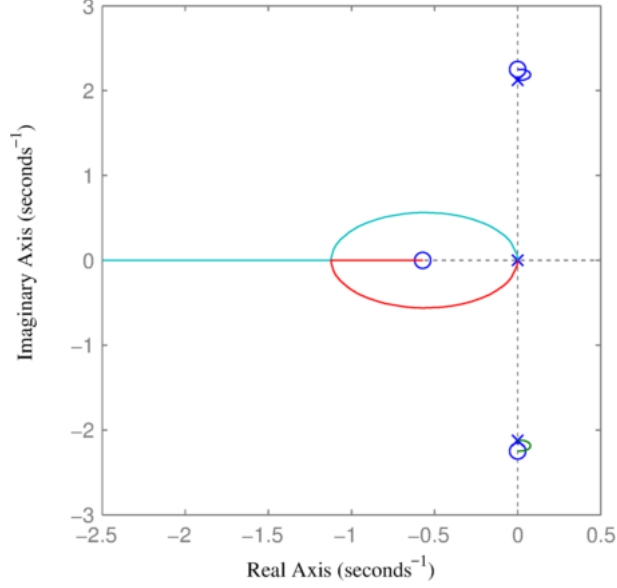


Figure 4. Root locus of OL transfer function for example system with PD control and with $\xi_{s1} = 0$. Note that there are 4 poles at the origin.

The transfer function from gimballed thrust to vehicle attitude angle, $\frac{\phi(s)}{\beta_e(s)}$, of the plant sets the position of the slosh poles and zeros and is given in Eq. (21) which is derived from the equations of motion (Eq. (1), Eq. (2), and Eq. (3)).

$$\frac{\phi(s)}{\beta_e(s)} = \frac{(c_2 - (c_2 m_{s1})/M + (k_4 l_{s1} m_{s1})/I)s^2 + c_2 \omega^2 + (k_3 k_4 m_{s1})/I}{(m_{s1}/M + (l_{s1}^2 m_{s1})/I - 1)s^4 + ((k_3 l_{s1} * m_{s1})/I - \omega^2)s^2} \quad (21)$$

The roots of the numerator and denominator can be solved for in terms of s^2 . Then the expression of l_{s1} for when the slosh pole and zero are co-located can be found by equating the two root expression and solving for l_{s1} . The assumption is made that $k_4 = k_3$. The resulting danger zone where the root locus is in the right half of the plane is given by Eq. 22 and Eq. 23. Note that the definition l_{s1} is positive if the slosh mass is behind the CG. This results expands the Greensite⁹ danger zone rear boundary to a point behind the CG instead of at the CG. The forward boundary is still at the center of percussion ahead of the CG. The difference from the Greensite derivation is that none of the terms are deemed negligible.

$$l_{s1} > \frac{-I}{M x_{c.g.}} \quad (22)$$

$$l_{s1} < \frac{F(M - m_{s1})}{M^2 \omega_{s1}^2} \quad (23)$$

For the example system, which is a big, short, and wide stage, the "danger zone" extends from 13.18m behind the CG to the center of percussion at 9.37m in front of the CG. For this set of parameters the Greensite definition of the danger zone which starts at the CG is not a good approximation.

C. Analysis Method

1. Stability Analysis

An LTI system analysis can be performed on the system for different values of slosh damping. For the example, the Bode diagram of the open loop system is show in figure 5. The slosh mode is at approximately 0.35 Hz which is about twice the 0dB cross over frequency of 0.17 Hz.

A Nichols diagram of the open loop response is shown in figure 6 with a disc margin (DM) threshold of 1 connecting the desired gain margin (GMD) of 6dB and phase margin (PMd) of $1/6\pi$ rad (30 deg) from

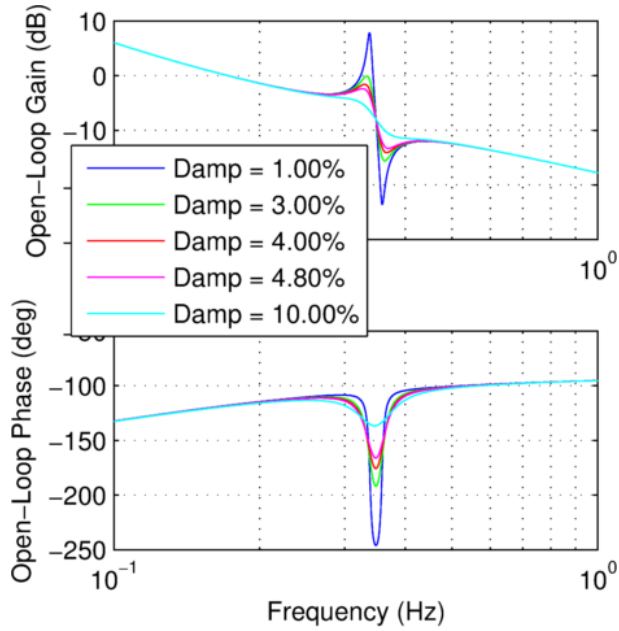


Figure 5. Bode of open loop response of example system with varying slesh mode damping.

the critical point at 0dB and $-\pi$ (-180 deg). The disc margin represents the radius of the response of the open loop transfer function ($G(\omega)$) in a gain and phase margin normalized Nichols plot and is computed by Eq. (24). A disc margin of 0.0 would correspond to a neutrally stable system and value of 1.0 would be the minimum acceptable value for a robust control design.

$$DM = \sqrt{\left(\frac{20\log_{10}(|G(\omega)|)}{GMd}\right)^2 + \left(\frac{(\angle G(\omega) \bmod 2\pi) - \pi}{PMd}\right)^2} \quad (24)$$

As can be seen by the encroachments of the disc margin in figure 6, the resulting LTI stability is a strong function of slesh damping. Since the slesh damping depends upon amplitude, the selection of amplitude at which damping is assumed will greatly affect the margin results. With a slesh mode damping of 1% the system is unstable. A damping of 4.8% corresponds to being right on the desired disc margin. The 3% damping response is an example where the gain and phase margins are ample but the system is not robust, showing the importance of using a combined metric such as the disc margin.

The presence of time delay, actuator dynamics, and filters to attenuate structural dynamics would have the effect of adding additional phase lag at the slesh frequencies and this effect is not represented in the example system. In the Nichols plot this would have the effect of bending the response to the left underneath the disc, sometimes making the slesh response come closer to the critical point from the bottom or from the bottom left.

2. TVC Angle to Slesh Displacement Gain

The gain of the transfer function from the thrust vector angle β_e to the slesh mass displacement z_{sj} due to the plant dynamics are shown in figure 7. Since this magnitude relationship is solely defined by the plant dynamics alone, it is not affected by any changes in the control system. As slesh damping decreases, the gain of z_{s1}/β_e increases. The consequence, is that for a given sized slesh limit cycle amplitude, a high gain means a small thrust vector angle amplitude. This simple fundamental relationship, along with the non-linear damping relationships enables the limit cycle assessment shown in the following section.

3. Predicted Thrust Vector Amplitude Limit Cycle

As demonstrated in figure 6, for a given slesh damping profile the stability of the system is a function of slesh amplitude, with the system being unstable at very low amplitudes, and stable at high amplitudes. For

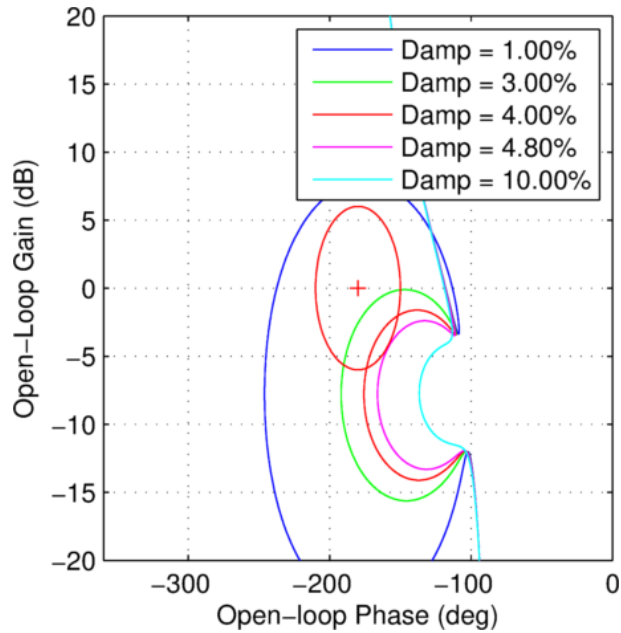


Figure 6. Nichols of open loop response of example system with varying slosh mode damping.

unforced conditions, a small unstable amplitude will grow in amplitude until damping is high enough that neutral stability is reached, resulting in a stable limit cycle. The damping corresponding neutral stability is associated with a slosh amplitude via α_{sj} , and can be subsequently related to the TVC angle limit cycle amplitude by using the inverse of z_{s1}/β_e transfer functions corresponding to the damping at neutral stability.

In order to properly account for margins in this process, the control system designer may choose both the permissible disc margin associated with the offending slosh mode as well as the acceptable TVC limit cycle. The process is as follows: Find the damping which corresponds with just meeting threshold disc margin $DM_{damping-threshold}$ (e.g. 4.8% damping for $DM = 1$ in the example system) and assume that the disc margin is degraded such that the system becomes neutrally stable. For time domain simulation, this could be accomplished with a gain change and time delay combination, but the frequency domain method above is not explicitly dependent on the method or means by which the stability margin is degraded. For example, if the gain and phase degradation occurs outside of the thrust vector angle to slosh displacement dynamics, (e.g. sensor dynamics, flight control system dynamics, or actuator dynamics) then the thrust vector angle to slosh displacement gain will not be affected. If the degradation does occur inside the thrust vector to slosh dynamics then the thrust vector to slosh gain will change, but it is conservative to assume it is unchanged if the slosh frequency is greater than the control frequency, since that situation involves a gain increase to cause the slosh mode to reach neutral stability, and that gain increase would correspond with a smaller TVC angle for a given slosh displacement. The other case, when slosh frequency is less than the control frequency is not likely in this class of launch vehicle control system designs since they are typically bandwidth constrained by the presence of structural dynamics at frequencies above the slosh frequencies.

The thrust vector angle to slosh displacement gain is a function of frequency and it is largest close to the slosh frequency and smaller further away. If a limit cycle were to develop due to non-slosh dynamics far away from the slosh frequency then slosh displacement participation will be very small. Increasing slosh damping in such as case would have very little effect in decreasing the magnitude of the limit cycle. To isolate slosh influenced parts of the response, a limit cycle threshold DM ($DM_{limit-cycle-threshold}$) value is chosen and all frequencies of the response which are below this threshold DM value are evaluated.

To review, the steps of the method are as follows:

1. Chose a TVC angle amplitude which is considered sufficiently small to be acceptable for degraded conditions.

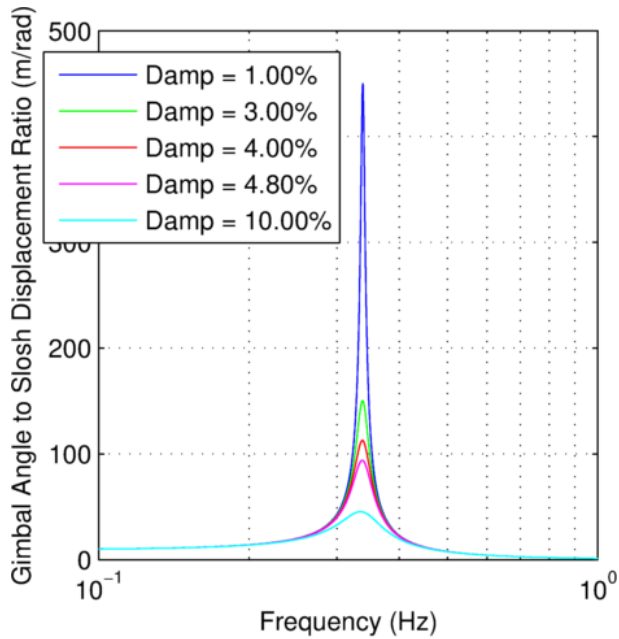


Figure 7. Thrust vector angle to slosh displacement gain for plant with varying slosh damping.

2. Chose $DM_{damping-threshold}$ and find the damping associated with being able to meet this margin. Determine the associated slosh displacement amplitude corresponding to this damping using the non-linear damping profile.
3. Chose $DM_{limit-cycle-threshold}$ and find the slosh related frequencies below this margin.
4. Multiply the slosh displacement amplitude by the inverse of the z_{s1}/β_e transfer function, for the determined frequency range, to find the predicted TVC limit cycle amplitude under the degraded conditions.
5. Check the maximum limit cycle amplitude over the frequency range against the chosen TVC threshold.

For the example system, a TVC limit of 0.5 degrees is chosen as an acceptably small limit cycle under degraded conditions, a $DM_{damping-threshold}$ of 1 is chosen for finding the slosh damping which just meets a minimum disc margin, and a $DM_{limit-cycle-threshold}$ of 1.1 is chosen for finding the slosh frequencies to use for evaluating the thrust vector limit cycle amplitude. For a very high slosh damping, none of the response would be less than $DM_{limit-cycle-threshold}$. In the example system, a damping of 4.8% (corresponding to a slosh amplitude of 0.48m) meets the $DM_{damping-threshold}$, and a frequency range between approximately 0.336 and 0.343 Hz corresponds to a disc margin less than the $DM_{limit-cycle-threshold}$. As figure 8 shows, the predicted limit cycle amplitude over the frequency range is on the order of 5 milliradians or approximately 0.3 degrees.

The limit cycle prediction can easily be tested in the linear system by degrading the gain and phase of the nominal system at the 4.8% damping level. Taking the minimum DM point at 0.34 Hz and degrading the control system with gain of 4.4 dB and a time delay of 170 ms results in a system with neutrally stable complex poles at that frequency. In time domain, the linear equation of motion can be modified to use the odd square law damping associated with α_{s1} to test the prediction of the limit cycle with non-linear damping. A simulation with perturbed initial conditions is shown in figure 9. As can be seen, the response grows to a limit cycle of approximately 0.48m of slosh displacement and 0.005 radian of TVC angle amplitude. In this case, the growth to the neutrally stable limit cycle took approximately 100s, a time period which could occur without appreciable mass property changes in lower thrust upper stages.

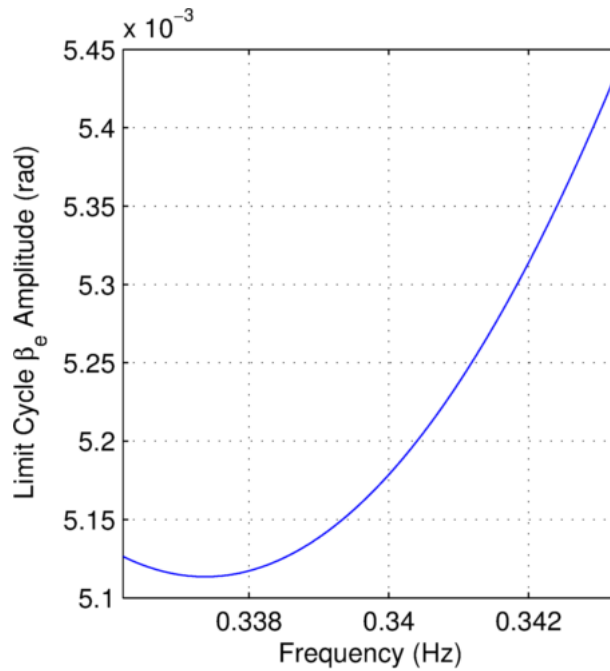


Figure 8. Limit cycle prediction of example system with a slosh damping of 4.8% and degraded gain and phase.

II. Conclusion

The analysis method presented herein is a method for accepting the control system stability characteristics of a liquid propelled space vehicle given predictions for the expected non-linear slosh damping. The analysis method can also be used to develop a damping requirements profile that can be used to design the needed slosh baffles for a new design. The values of the TVC threshold, $DM_{damping-threshold}$ and $DM_{limit-cycle-threshold}$ are a choice to the control system designer. The values chosen for the example system (0.5 degrees, 1.0, and 1.1) can be considered a reasonable conservative set of values. The disc margin values can be argued to be over-conservative since for other dynamics, such as aerodynamics or rigid body dynamics, a DM of 1.0 is considered acceptable for a nominal system, and there is no expectation that a limit cycle of sufficiently small consequence would occur should the full DM be lost.

While the analysis herein predicts the homogeneous system response, a more complete analysis of the disturbance response of the system is important when determining the acceptability of candidate baffle designs. A non-linear time varying Monte Carlo analysis with the non-linear damping profile should also be done to ensure acceptable performance. It is possible that the unforced limit cycle is small, but under forced conditions, motion can be increased to larger levels. It is also important to look at the magnitude of the slosh motion even if TVC motion is small.

Acknowledgments

Research supported by NASA contract number NNM12AA41C. The helpful discussions with John Wall are greatly appreciated.

References

- ¹Bjelde, B., Vozoff, G., and Shotwell, G., "The Falcon 1 Launch Vehicle: Demonstration Flights, Status, Manifest and Upgrade Path," *SSC-07-III-6, 21st Annual AIAA/USU Conference on Small Satellites*, 2007.
- ²Abramson, H., *The Dynamic Behavior of Liquids in Moving Containers*, NASA SP-106, 1967.
- ³Dodge, F., *The New "Dynamic Behavior of Liquids in Moving Containers"*, Southwest Research Inst., 2000.
- ⁴Miles, J., "Ring Damping of Free Surface Oscillations in a Circular Tank," *Journal of Applied Mechanics*, Vol. 25, No. 2, 1958, pp. 274–276.

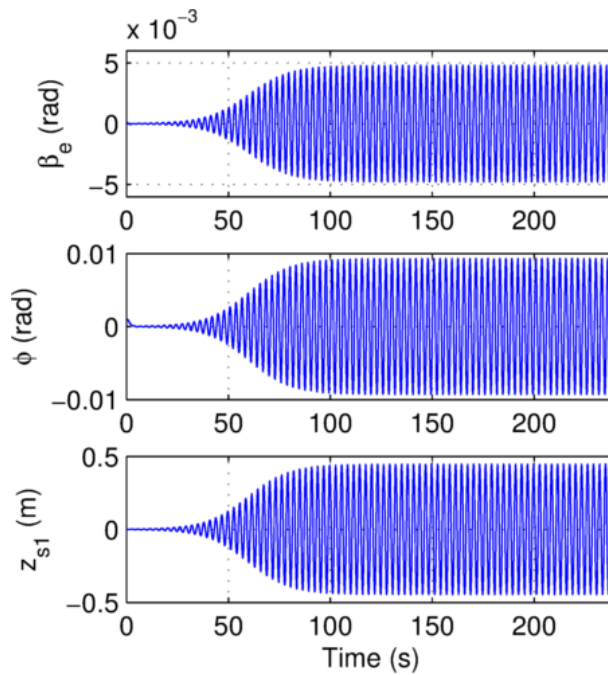


Figure 9. Time domain limit cycle demonstration of example system with a slosh damping of 4.8% and degraded gain and phase.

⁵Yang, H. and West, J., “Validation of High-Resolution CFD Method for Slosh Damping Extraction of Baffled Tanks,” *52nd AIAA/SAE/ASEE Joint Propulsion Conference, AIAA Propulsion and Energy Forum, (AIAA 2016-4587)*, 2016.

⁶Lee, A., Strahan, A., Tanimoto, R., and Casillas, A., “Preliminary Characterization of the Altair Lunar Lander Slosh Dynamics and Some Implications for the Thrust Vector Control Design,” *AIAA Guidance, Navigation, and Control Conference 2 - 5 August 2010, Toronto, Ontario Canada*, 2010.

⁷Frosch, J. and Vallely, D., “Saturn AS-501/S-IC Flight Control System Design,” *Journal of Spacecraft*, Vol. 4, No. 8, 1967, pp. 1003–1009.

⁸Bauer, H., “Stability Boundaries of Liquid-Propelled Space Vehicles with Sloshing,” *Journal of Spacecraft*, Vol. 1, No. 7, 1963, pp. 1583–1589.

⁹Greensite, A., “Analysis and Design of Space Vehicle Flight Control Systems, Volume I - Short Period Dynamics,” Tech. rep., NASA CR-820, 1967.

¹⁰Bauer, H., “Nonlinear Mechanical Model for the Description of Propellant Sloshing,” *AIAA Journal*, Vol. 4, No. 9, 1962, pp. 1662–1668.

¹¹Peterson, L., Crawley, E., and Hansman, R., “Nonlinear Fluid Slosh Coupled to the Dynamics of a Spacecraft,” *AIAA Journal*, Vol. 27, No. 9, 1989, pp. 1230–1240.

¹²de Weerd, E., van Kampen, E., van Gemert, D., Chu, Q., and Mulder, J., “Adaptive Nonlinear Dynamic Inversion for Spacecraft Attitude Control with Fuel Sloshing,” *AIAA Guidance, Navigation and Control Conference and Exhibit 18 - 21 August 2008, Honolulu, Hawaii*, 2008.

¹³Dennehy, C., Lebsack, K., and West, J., “GNC Engineering Best Practices For Human Rated Spacecraft Systems,” Tech. rep., NASA/TM-2008-215106, 2008.

¹⁴Orr, J. and Hall, C., “Parametric Optimization of Ares I Propellant Slosh Characteristics Using Frequency Response Criteria,” *AIAA Guidance, Navigation and Control Conference*, 2009.

¹⁵Gelb, A. and Vander Velde, W., *Multiple-Input Describing Functions and Nonlinear System Design*, McGraw-Hill, Inc., 1968.

¹⁶Craig, R. and Kurdila, A., *Fundamentals of Structural Dynamics 2nd Edition*, John Wiley and Sons, Inc., Hoboken, New Jersey, 2006.